

# Impact of Dynamic Traffic on Vehicle-to-Vehicle Visible Light Communication Systems

Farah Mahdi Alsalamy , *Student Member, IEEE*, Olivier C.L. Haas , *Senior Member, IEEE*, Ahmed Al-Kinani, Cheng-Xiang Wang , *Fellow, IEEE*, Zahir Ahmad , and Sujan Rajbhandari , *Senior Member, IEEE*

**Abstract**—In this article we studies the impact of dynamic vehicular traffic density on the signal-to-noise-ratio and the associated bit-error-rate (BER) performance of vehicle-to-vehicle visible light communication (V2V-VLC) systems. The article uses traffic data from the M42 and M6 motorways in the U.K. to investigate the probability of coexistence of other vehicles in the adjacent lanes, which induce interference and act as potential reflectors. The results show that the probability of coexistence of other vehicles in the adjacent lanes is lane-independent and it increases during the rush hours to 90%, while it decays to less than 10% during the off-peak and early morning hours. The intervehicular distance and the BER performance vary widely between different lanes and different periods of the day. The results also show that the BER performance of V2V-VLC system with non-line-of-sight (NLOS) component and with LOS component are comparable at rush hours. However, high BER values are predicted during the off-peak hours for NLOS components of the channel.

**Index Terms**—Dynamic traffic conditions, dynamic vehicular traffic density, vehicular communication channel model, vehicular communications, visible light communication (VLC).

## I. INTRODUCTION

**R**OAD accidents, mostly caused by human errors, are one of the main causes of accidental death in the world [1], [2].

Manuscript received 29 December 2020; revised 31 March 2021 and 2 June 2021; accepted 14 July 2021. Date of publication 17 August 2021; date of current version 26 August 2022. This work was supported by a self-funded Ph.D. programme at Coventry University, U.K. The work of Olivier C.L. Haas was supported by Assured CAV Parking, innovate-U.K. under Grant 105095. The work of Cheng-Xiang Wang was supported in part by the National Natural Science Foundation of China (NSFC) under Grant 61960206006 and in part by the European Commission (EU) H2020 RISE TESTBED2 project under Grant 872172. (*Corresponding author: Sujan Rajbhandari.*)

Farah Mahdi Alsalamy is with the Department of Electronic Engineering, University of York, York YO10 5DD, U.K. (e-mail: farah.al-sallami@york.ac.uk).

Olivier C.L. Haas is with the Institute for Clean Growth and Future Mobility, Coventry University, coventry CV1 5FB, U.K. (e-mail: csx259@coventry.ac.uk).

Ahmed Al-Kinani is with the MMX Communications Services Limited, Birmingham B90 4SH, U.K. (e-mail: aalkinani@mmxcomms.com).

Cheng-Xiang Wang is with the National Mobile Communications Research Laboratory, School of Information Science and Engineering, Southeast University, Nanjing 210096, China, and also with the Purple Mountain Laboratories, Nanjing 211111, China, China, and the School of Engineering and Physical Sciences, Heriot-Watt University, Edinburgh EH14 4AS, U.K. (e-mail: chxwang@seu.edu.cn).

Zahir Ahmad is with the Faculty of Engineering, Environment and Computing, Coventry University, Coventry CV1 5FB, U.K. (e-mail: ab7175@coventry.ac.uk).

Sujan Rajbhandari is with the School of Computer Science and Electronic Engineering, Bangor University, Bangor LL57 1UT, U.K. (e-mail: sujan@ieee.org).

Digital Object Identifier 10.1109/JSYST.2021.3100257

Traffic management technologies and systems exploiting intelligent transport system (ITS) aim to reduce human errors. Based on ITS, many innovative systems have been proposed, such as vehicle-to-vehicle (V2V), vehicle-to-infrastructure (V2I), vehicle-to-pedestrian (V2P), and most recently vehicle-to-everything (V2X) communications [2]–[5]. Such communication aims to improve drivers' awareness and enable connected and autonomous safety features on vehicles.

The literature suggests that wireless communication technologies, such as dedicated short-range communications, IEEE 802.11p, LTE-V2V, 5G, and more recently 6G can enable connectivity between vehicles and with the infrastructure [4], [6]. The allocated bandwidth of the suggested technologies, which use the radio frequency (RF) spectrum, is limited [7]. Hence, it is expected for this technology to suffer from interference and bandwidth scarcity [7]–[9]. Visible light communication (VLC) is proposed as a complementary technology to reduce the bandwidth congestion as well as free up the RF spectrum for critical applications [3], [8]–[10].

VLC utilizes existing street-lights, traffic lights, vehicles' headlights, and vehicles' taillights to transmit traffic data between vehicles and interact with the infrastructure. In addition, due to the directional nature of light sources, VLC incurs less interference compared to RF [2], [9], [11].

The dynamic nature of the vehicular communication system results in a high probability for VLC links to be interrupted due to interference and reflection from the adjacent vehicles in the other lanes. Interference from neighboring artificial light sources of the adjacent vehicles increases the shot noise [2], [11], [12]. Furthermore, the reflected light from the adjacent vehicles in the neighboring lanes disperses the received signal pulses and consequently introduces the inter-symbol interference problem, which limits data rates. Hence, it is important to investigate the statistics of the existence of other vehicles in the adjacent lanes. In the following section, we provide related works that discussed the impact of interference and reflection from natural and artificial sources on vehicular VLC (VVLC) systems, which include V2V, V2I, V2P, and V2X communications.

## A. Related Works

The impact of interference from natural optical sources has been investigated in [13]–[16]. The impact of the sunlight interference on VLC system performance studied in [13] indicated that there is more than 20 dB variation in background noise

powers between the lower levels in the early morning and its peak during noon. Therefore, a diversity receiver with the selective combining technique was proposed which improved signal-to-noise-ratio (SNR) by 5 dB. The study in [14] evaluated the degradation in SNR, data rate, and BER performance of VLC systems under the presence of sunlight in different locations. The study estimated the solar irradiance variations during different hours of the day and different seasons. The results showed that VLC link with a data rate of 1 Gbps can be achieved in presence of sunlight without optical filter while blue filters offer 6.47 dB improvement in SNR. Likewise, [15] shows that an optical filter can block the out-of-band ambient lights with an incident angle greater than  $30^\circ$ . The study in [16] accounted for sunlight irregularities and identified the maximum and minimum solar irradiation for every day of the year. The results showed that maximum radiation reduces the transmission distance by 5 m for binary pulse amplitude modulation scheme.

However, only limited research activities investigated the impact of interference from artificial light sources in VVLC systems. The work reported in [17] considered the impact of interference due to vehicles in the adjacent lanes on the performance of VVLC for Platoon scenario. The results showed that the performance decays when the rate of arrival of vehicles in the adjacent lanes increases. The work in [9] highlighted the impact of interference at high traffic density in the VLC and RF systems. According to [9], VLC has a low interference level and limited transmission range. Therefore, the study suggested a hybrid VLC/RF-enabled Vehicular Ad-hoc Network (VANET). VLC technology was utilized due to broad bandwidth, high power efficiency, and relatively low reflection. RF was utilized to support longer transmission ranges. The work in [8] considered VLC technology to tackle the interference and delay in RF-based V2V systems under dense traffic conditions. The study proposed VLC for dual functions of communications and distance estimation.

A geometry-based analytical method to study V2V VLC (V2V-VLC) channel was considered in [18] and [19]. The work in [18] investigated the effect of the light reflection from the road surface and road dirt. However, the study utilized a tungsten-halogen headlight beam pattern, which may not be applicable for V2V-VLC systems that use light-emitting diode (LED) light sources. The results showed that wet roads increase the received power of the reflection and hence increase the transmission distance. The study in [18] was extended in [19] to increase the transmission data rate of V2V-VLC link using a multiple-input multiple-output (MIMO) system. The  $2 \times 2$  MIMO system achieved a data rate of 4 Mbps for a transmission distance of 40 m. These studies, however, did not consider the reflection from the adjacent vehicles which can be significant, particularly in dense traffic conditions.

A two-dimensional (2-D) geometry-based stochastic model (GBSM) with two rings and an ellipse to investigate the V2V-VLC channels was proposed in [3]. The study considered line-of-sight (LOS) and reflected power from surrounding vehicles and roadsides in dynamic V2V-VLC environments. The results showed that the received power due to the reflection and scattering from roadsides and vehicles in the dynamic V2V-VLC

channel is less than the received power for the LOS component by at least two orders of magnitude. The study in [3] was extended in [20] to consider the asymmetrical radiation pattern of vehicles' headlights. The study used a 3-D GBSM with two spheres and an ellipsoid to model the V2V-VLC channel. The results highlighted the importance of considering the 3-D radiation pattern of the vehicle's headlights. Likewise, the study in [21], used the GBSM to study the received power of the direct LOS and reflections from surrounding vehicles in dynamic V2V-VLC channel. The study showed that the variation in the relative speed of vehicles impacts the reflected power more than the LOS power. The direction of the vehicle's motion affects the received power from the LOS component more than the received power of the reflection component.

VVLC systems are affected by multiple variables including radiation pattern, weather conditions, interference from artificial and natural light sources, traffic conditions, coating and color of cars as well as the condition of road surfaces (wet or dry). However, these variables are independent. Hence, a universal model that considers the impact of these variables can be found by combining the impact of independent variables. The effect of the radiation pattern on VVLC was considered in [22], where analytical models that can describe the radiation pattern of headlamp from different manufacturers and designs were proposed. The impact of different weather conditions and specular reflections from surrounding vehicles and road was considered in [23]. The study showed that the propagation path loss due to the intervehicle distance variation is significantly higher than the attenuation due to adverse weather condition (e.g., dense fog). In addition, the reflections from street furniture have a marginal impact compared to the reflection from vehicles due to the modest reflectivity of other surfaces. Therefore, in this study, we focus on the reflection from surrounding vehicles in the adjacent lanes and dynamic behaviors of the VVLC channel due to traffic conditions during different times of the day.

The previous studies identified the impact of the interference and reflection on VVLC channel. However, none of these studies investigated the statistics of the existence of other vehicles in the adjacent lanes, which can significantly affect the levels of interference and reflection.

## B. Motivation and Original Contribution

Surrounding vehicles with a body characterized by a relatively high reflectivity are the closest reflective objects to the V2V-VLC link. In addition, interference from adjacent vehicles light sources increases the shot noise [11], [12], [24]. However, due to the dynamic nature of traffic, which varies during different periods of the day, the presence of the adjacent vehicles changes with the traffic flow. Therefore, our motivation is to evaluate the effect of interference and reflection from the surrounding vehicles in the adjacent lanes and study their impact on V2V-VLC performance during different times of the day based on real traffic measurement data.

The novelty and original contributions of this article are as follows:

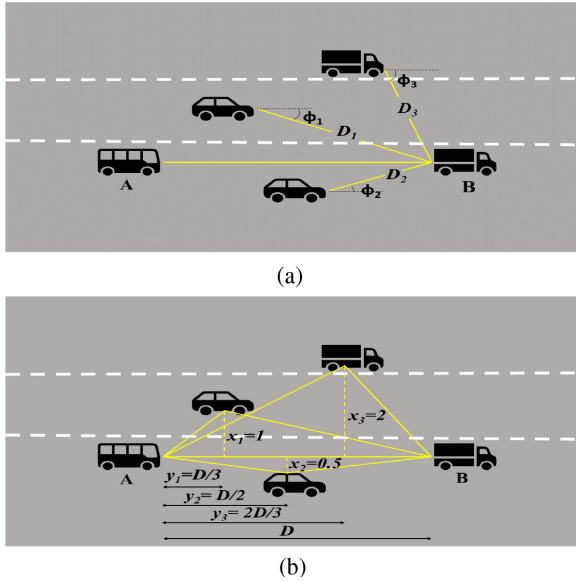


Fig. 1. Typical communication link between two vehicles travelling on a three-lane motorway and coexistence of other vehicles in the adjacent lanes which act as (a) interference sources and (b) reflectors.

- 1) Use traffic measurements to estimate the probability of coexistence of other vehicles in the adjacent lanes. This is expected to be an important factor to examine the performance of vehicular communication systems regardless of the communication technologies in use.
- 2) Consider the radiation pattern model for low-beam and high-beam headlights to study the LOS and non-LOS (NLOS) components of the V2V-VLC channel.
- 3) Study the impact of dynamic vehicular traffic density on V2V-VLC channel SNR and BER performance in different Lanes.

The rest of this article is organized as follows. The V2V-VLC link performance is presented in Section II. The V2V-VLC channel gain is explained in Section III. The probability of coexistence of other vehicles in the adjacent lanes is presented in Section IV. Numerical results are discussed in Section V. Finally, Section VI concludes this article.

## II. V2V-VLC LINK PERFORMANCE

The proposed V2V-VLC link scenario is shown in Fig. 1. The transmitter vehicle A and the receiver vehicle B drive on a motorway in the presence of other vehicles in the adjacent lanes. The surrounding vehicles can act as ambient light interference sources and/or as potential reflectors.

If  $x(t)$  is the transmitted optical signal, then the received signal  $y(t)$  is given by [25]

$$y(t) = \gamma h(t) \otimes x(t) + n(t). \quad (1)$$

Here,  $\otimes$  refers to convolution operation,  $\gamma$  denotes the receiver's responsivity,  $h(t)$  is the channel impulse response and  $n(t)$  is the additive white Gaussian noise (AWGN) with zero mean and variance  $\sigma_T^2$ .

The AWGN is caused by thermal and ambient noises. The total noise variance  $\sigma_T^2$  is given by [18]

$$\sigma_T^2 = \sigma_{shot}^2 + \sigma_{th}^2 \quad (2)$$

where  $\sigma_{shot}^2$  and  $\sigma_{th}^2$  are the shot and thermal noise variances, respectively.

The thermal noise variance is given by [11]

$$\sigma_{th}^2 = \frac{8\pi K_k T_k C_{pd} A_r I_2 B_w^2}{G_\nu} + \frac{16\pi^2 K_k T_k \Gamma C_{pd}^2 A_r^2 I_3 B_w^3}{g_m} \quad (3)$$

where  $K_k$  denotes the Boltzmann's constant,  $T_k$  is the absolute temperature,  $C_{pd}$  refers to the fixed capacitance of a photodiode per unit area,  $A_r$  is the active area of the receiver,  $I_2$  and  $I_3$  are the noise bandwidth factors,  $B_w$  is the noise bandwidth,  $G_\nu$  indicates the open-loop voltage gain,  $\Gamma$  is the FET channel noise factor and  $g_m$  denotes FET transconductance.

The background daylight and the artificial light (such as the lights from the adjacent vehicles) are the main sources of ambient noise in V2V-VLC systems [18]. However, daylight is the dominant source of ambient noise [18], which peaks only at morning hours [13]. During the night, the artificial light sources of the adjacent vehicles are the main sources of ambient noise. The incident luminous flux of the ambient noise induces a shot noise, which is given by [13]

$$\sigma_{shot}^2 = 2q(P_R + LP_I)\gamma B_w + 2qI_{bg}I_2 B_w \quad (4)$$

where  $q$  is the electron charge,  $P_R$  is the received power,  $L$  describes the probability of coexistence of other vehicles in the adjacent lanes,  $P_I$  is the interference power from vehicles in adjacent lanes as illustrated in Fig. 1(a),  $I_{bg}$  is the current induced by the ambient light sources.

The received power  $P_R$  in V2V-VLC is a linear superposition of the power from LOS and NLOS paths. The received power  $P_R$  is calculated from the transmitted power  $P_T$  as [11]

$$P_R = P_T H(0) \quad (5)$$

where  $H(0)$  is the dc channel gain given as

$$H(0) = \int_{-\infty}^{\infty} h(t) dt. \quad (6)$$

The path loss of the channel equals the dc gain of the channel  $H(0)$  measured in decibels (dB). Therefore, the SNR at the receiver is given by [24]

$$\text{SNR} = \frac{\gamma^2 P_R^2}{\sigma_T^2}. \quad (7)$$

The ON-OFF keying (OOK) modulation scheme is widely considered as a competent candidate in VVLC systems that use intensity modulation/direct detection (IM/DD) schemes because it is simple and resilient to ambient noise and the nonlinearity distortion of the LED [11], [18]. Therefore, considering OOK modulation scheme, the BER of the system is given by [11]

$$\text{BER} = Q(\sqrt{\text{SNR}}) \quad (8)$$

where

$$Q(y) = \frac{1}{\sqrt{2\pi}} \int_0^{\infty} e^{-y^2/2} dy. \quad (9)$$

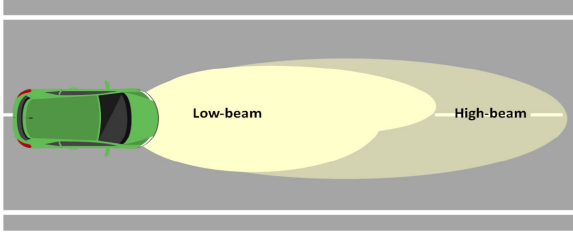


Fig. 2. Schematic (not to scale) of high-beam and low-beam patterns projection on the road surface.

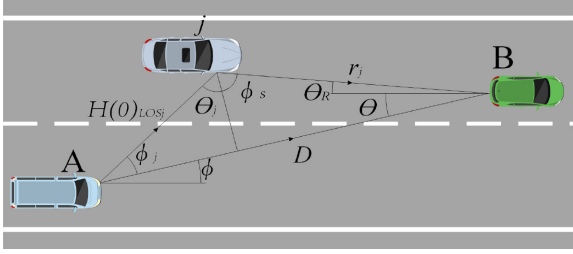


Fig. 3. The LOS and NLOS propagation paths of the optical signal between the transmitter vehicle A and the receiver vehicle B.

The equations (5), (7), and (8) show that to establish the communication performance, the dc channel gain is required. In the next section, we present the theoretical study of V2V-VLC channel gain.

### III. V2V-VLC CHANNEL GAIN

To characterize the channel gain, we consider the radiation pattern of vehicles headlights. Vehicles use low-beams at high traffic density when the intervehicular distance is short. Based on ECE R112 regulation, the radiation pattern of low-beam headlights is asymmetrical, directed toward road surface and with shorter luminous range to avoid driver blindness by the direct light from vehicles coming from the opposite direction [26]–[28]. At low traffic density when the intervehicular distance is longer, vehicles use high-beam headlights. The high-beam headlights radiation pattern is not restricted by the ECE R112 regulation [27]. Therefore, the Lambertian model is considered to describe the symmetrical radiation pattern of high-beam headlights with LED. A schematic of high-beam and low-beam patterns projection on the road surface is illustrated in Fig. 2.

The LOS and NLOS propagation paths of the optical signal between the transmitter vehicle A and the receiver vehicle B are illustrated in Fig. 3. The dc channel gain of LOS path for the Lambertian source is given by [28]

$$H_{\text{LOS}}(0) = \frac{A_r(m+1)}{2\pi D^2} \cos^m(\phi) \cos(\theta) \quad (10)$$

where  $D$  is the intervehicular distance,  $\phi$  is the irradiance angle,  $\theta$  is the incident angle at the PD, as illustrated in Fig. 3, and  $m = \frac{-0.6931}{\ln(\cos(\Psi_{1/2}))}$  is the Lambertian order and  $\Psi_{1/2}$  is the half-power angle of the radiation.

In this article, we use an empirical radiation model of the source as outlined in [29]. This model describes the angular distribution of the asymmetric radiation intensity pattern of the low-beam headlight. Accordingly, the LOS channel path loss (in dB) is given by [29]

$$P_{\text{LOS}} = \alpha + \delta - 10\beta \log_{10}(D+1) + \epsilon \cos\left(\frac{2\pi(\phi+90)}{\omega}\right) \quad (11)$$

where the numerical constant ( $\alpha = 695.3$ ,  $\delta = -717.3$ ,  $\beta = 4.949$ ,  $\epsilon = 63.13$ , and  $\omega = 173$ ) were determined from the empirical measurements of vehicle headlight using the nonlinear least square method [29].

Considering a Lambertian diffuse reflection from vehicle surfaces [30], [31], the channel gain from the reflectors is given as

$$H_{\text{refa}}(0) = \sum_{j=1}^N \frac{\rho H_{\text{LOS}_j}(0)}{2\pi r_j^2} \cos(\phi_s^j) \cos(\theta_R^j) \quad (12)$$

where  $H_{\text{LOS}_j}(0)$  is the LOS dc channel gain from the source to the  $j$ th reflector, as illustrated in Fig. 3,  $N$  is the total number of reflectors,  $r_j$  is the distance from the  $j$ th reflector to the receiver,  $\rho$  is the reflective index of the reflection surface,  $\theta_R$  is the incidence angle at the receiver and  $\phi_s$  is the irradiance angle with respect to the normal to the reflector. The power received from reflections is  $P_{R_{\text{ref}}} = P_T L H_{\text{ref}}(0)$ .

The performance of the V2V-VLC link is affected by the existence of other vehicles in the adjacent lanes, which induce additional noise and multipath propagation. Therefore, in the Section IV, we study the probability of coexistence of other vehicles in the adjacent lanes.

### IV. PROBABILITY OF COEXISTENCE OF OTHER VEHICLES IN THE ADJACENT LANES

In this article, we use traffic measurements to calculate the probability of co-existence of other vehicles in the adjacent lanes. We determine the existence of vehicles from traffic flow and road occupancy data.

To calculate the coexistence of other vehicles in the adjacent lanes, we first define the event  $f_k$ , which indicates that the number of vehicles in the  $k$ th lane ( $k = 1, 2, 3$  for the left-hand, middle, and the right-hand lanes, respectively) is larger than one. A logic 1 is assigned to the event  $f_k$  to indicate that the traffic flow in the  $k$ th lane ( $\text{flow}_k$ ) is larger than one, and hence the number of vehicles is larger than one, and 0 otherwise. Then, we calculate the event  $R_i$  of having at least two vehicles in any two lanes, as described in Algorithm 1.

However, the probability of co-existence of other vehicles in the adjacent lanes is reinforced by the increasing road occupation percentages  $O_k$ , which measures the time duration of a vehicle occupying the  $k$ th lane. Therefore, the probabilities of coexistence of other vehicles in the adjacent lanes  $L_k$  is given as a product of the event of having two vehicles in any two lanes  $R_i$  and the percentages that these vehicles occupy the road for a longer time  $O_k$ , which are given by

$$L_3 = R_i \times \left(\frac{O_2 + O_1}{2}\right) \quad (13)$$

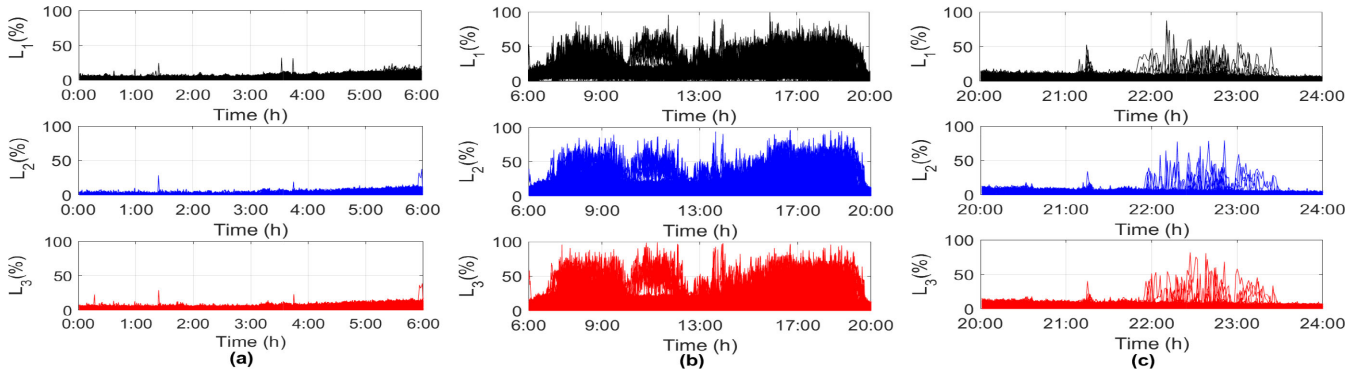


Fig. 4. Probability of coexistence of other vehicles in the adjacent lanes during (a) the late night and early morning hours (00:00–06:00) (b) the rush hours (06:00–20:00), and (c) the night hours (20:00–24:00).

---

**Algorithm 1:** The Event of Co-existence of Other vehicles in the Adjacent Lanes at Time Instant  $i$  (in seconds).

---

**Result:**  $R_i$

**while**  $i \neq 0$  **do**

**if**  $flow_1 \geq 1$  **then**  $f_1 = 1$ ; **else**  $f_1 = 0$ ;  
**if**  $flow_2 \geq 1$  **then**  $f_2 = 1$ ; **else**  $f_2 = 0$ ;  
**if**  $flow_3 \geq 1$  **then**  $f_3 = 1$ ; **else**  $f_3 = 0$ ;  
 $R_i = f_3 \& f_2 \parallel f_3 \& f_1 \parallel f_2 \& f_1$ ;

---

$$L_2 = R_i \times \left( \frac{O_3 + O_1}{2} \right) \quad (14)$$

$$L_1 = R_i \times \left( \frac{O_3 + O_2}{2} \right). \quad (15)$$

Then, the distribution that describes the probability of the coexistence of other vehicles in the adjacent lanes can be calculated using the distribution of  $L_k$ .

## V. DATA PROCESSING, RESULTS, AND DISCUSSION

### A. Traffic Data Processing

Traffic flow and road occupancy were obtained from data collected from the multiple-loop sensors on the M6 and M42 motorways in the U.K. The data were collected on the 21, 24, and 28 November 2017 on the M42, and on 6, 7, and 8 December 2017 on the M6. Consecutive 60 min of traffic data were collected over 24 h period starting at midnight. The measurements for the M42 and M6 were collected using 318 and 154 sensors, respectively. The traffic flow and road occupancy per lane are measured when vehicles enter and exit the sensor loop on the road. The M42 is a smart motorway with enforced variable speed limits and hard shoulder running at rush hours, whereas the M6 was, at the time the data were collected, a standard motorway. However, in our analysis, we considered three lanes excluding the hard shoulder lane. We did not observe a difference between the statistics of both motorways at this particular dataset. Therefore, the resulting models were averaged to improve the model generalizability.

In order to study the statistics of the event of the coexistence of other vehicles in the adjacent lanes during different periods of time, we analyze the probability of the coexistence of other vehicles in the adjacent lanes versus time in Fig. 4. We consider the traffic during a day in three lanes; the right-hand lane (Lane 3), middle lane (Lane 2), and left-hand lane (Lane 1). According to the traffic density, we consider three periods 00:00–06:00, 06:00–20:00, and 20:00–24:00. The time periods 00:00–06:00, and 20:00–24:00 have low traffic density. The time period 06:00–20:00 has high traffic density. Depending on the analysis described in Section IV, the probability of the coexistence of other vehicles in the adjacent lanes  $L_k$  during the low-density traffic during the late night and early morning hours from 00:00 to 06:00 is presented in Fig. 4(a). The figure shows that the probabilities of the coexistence of other vehicles in the adjacent lanes are initially below 10%, in the three lanes. Then, it starts to increase gradually after 03:00, exceeding 20%. Therefore, we use the time window between 00:00 and 03:00 to study the off-peak probability of the coexistence of other vehicles in the adjacent lanes in the rest of this article.

The probability of the coexistence of other vehicles in the adjacent lanes during the rush hours (06:00–20:00) is presented in Fig. 4(b). The figure shows that the probability of the coexistence of other vehicles in the adjacent lanes increases significantly ( $> 60\%$ ) after 7:00. These high probability values can be noticed over the entire time window. It can reach 90% between 16:00 and 19:00. Therefore, we use this time window to study the probabilities of the coexistence of other vehicles in the adjacent lanes when the traffic density has the highest values.

The probability of the coexistence of other vehicles in the adjacent lanes during the night hours (20:00–24:00) is presented in Fig. 4(c). The figure shows that the probability of the coexistence of other vehicles in the adjacent lanes is below 10% between 20:00 and 22:00, for the three lanes. During the time window 22:00–23:00, the probability of the coexistence of other vehicles in the adjacent lanes increases, but it does not exceed 60%. The probability of the coexistence of other vehicles decreases again to below 10% at the last hour of the day.

To establish the distribution that closely estimates coexistence of other vehicles in the adjacent lanes, we performed a cumulative distribution function (CDF) curve fitting method with

TABLE I  
 PARAMETERS OF DIFFERENT DISTRIBUTIONS THAT ARE EXPECTED TO DESCRIBES  $L$  AND  $D$ 

Time	Lane	Distribution	Parameters of $L$					Parameters of $D$				
			Mean Value (m)	$\mu_l$	$\mu_l$ estimation error (%)	$\delta_l$	$\delta_l$ estimation error(%)	Mean Value (m)	$\mu_d$	$\mu_d$ estimation error (%)	$\delta_d$	$\delta_d$ estimation error(%)
00:00-03:00	left (1)	log-normal	3.74	1.21	0.41	0.46	0.29	57.2	3.72	0.45	0.80	0.32
	middle (2)		2.55	0.78	0.98	0.56	0.69	67.1	3.82	0.44	0.87	0.31
	right (3)		3.61	1.18	0.34	0.45	0.24	109.8	4.35	0.64	0.83	0.45
	left (1)	Nakagami	3.7	1.56	1.8	16.2	11.67	62.1	0.5	0.33	6032	4844
	middle (2)		2.6	0.94	2.0	8.7	15.7	73.3	0.45	0.26	8770	6630
	right (3)		3.6	1.6	1.6	15.1	9.3	107.9	0.59	0.54	17131	1723
	left (1)	Normal	3.7	3.7	1.4	1.6	1.0	57.2	57.2	29.8	52.3	21.0
	middle (2)		2.5	2.5	2.6	1.5	1.8	67.1	67.1	33.2	65.3	23.4
	right (3)		3.6	3.6	1.2	1.5	0.8	104.0	104.0	78.9	61.2	43.3
	left (1)	Exponential	3.7	3.7	3.3	-	-	57.5	57.5	32.7	-	-
	middle (2)		2.5	2.5	4.4	-	-	67.1	67.1	34.1	-	-
	right (3)		3.6	3.6	2.8	-	-	104.0	104.0	81.0	-	-
16:00-19:00	left-hand (1)	log-normal	19.9	2.71	0.30	0.70	0.25	7.8	1.35	0.45	1.18	0.31
	middle (2)		16.7	2.44	0.35	0.87	0.20	3.9	0.81	0.42	1.05	0.29
	right (3)		17.4	2.58	0.45	0.74	0.21	2.5	0.50	0.27	0.90	0.39
	left (1)	Nakagami	19.3	0.73	0.38	515	262	11.9	0.2	0.10	325	256
	middle (2)		15.9	0.58	0.28	380	205	8.3	0.2	0.09	169	148
	right (3)		17.8	0.64	0.31	457	235	5.2	0.2	0.11	63.3	57.7
	left (1)	Normal	18.9	18.9	5.4	12.5	3.8	8.6	8.6	6.0	15.8	4.2
	middle (2)		15.6	15.6	4.5	11.7	3.9	5.1	5.1	4.8	11.9	3.4
	right (3)		17.1	17.1	5.2	12.7	3.7	3.1	3.1	6.0	7.3	2.2
	left (1)	Exponential	18.9	18.9	8.27	-	-	8.6	8.6	3.27	-	-
	middle (2)		15.6	15.6	6.4	-	-	5.1	5.1	2.0	-	-
	right (3)		17.2	17.2	7.0	-	-	3.1	3.1	1.3	-	-

normal, log-normal, exponential, and Nakagami distributions. Table I provides parameters of different distributions that are expected to fit the coexistence of other vehicles in the adjacent lanes for the three lanes during 00:00–03:00 and 16:00–19:00. Distribution fit is measured by the standard error values of the distribution's parameters, which achieve the least estimation errors. The table shows that among Normal, log-normal, Nakagami, and exponential distributions, the log-normal distribution provides a close fit to the coexistence of other vehicles in the adjacent lanes because it has the least standard error values. Therefore, the probability of coexistence of other vehicles in the adjacent lanes is given by

$$P_L(l) = \frac{1}{\delta_l \sqrt{2\pi}} \frac{1}{l} \exp\left(-\frac{(\ln(l) - \mu_l)^2}{2\delta_l^2}\right). \quad (16)$$

The distribution parameters  $\mu_l$  and  $\delta_l$  are given in Table I. The CDF curve fitting of the coexistence of other vehicles in the adjacent lanes is illustrated in Fig. 5 during off-peak hours 00:00–03:00 and during rush hours 16:00–19:00, respectively. The figure shows that the CDF curves fit a log normal distribution.

The table shows that the probability of the coexistence of other vehicles in the adjacent lanes for the three lanes are very close during a particular period of time. However, the mean values vary widely between the two periods. The mean values are between 3.75% – 2.55% during the off-peak hours, while they are between 19.9% – 16.7% during the rush hours. The results show a large variation between the probability values during the rush and off-peak hours but the majority of probability values does not exceed 20% and 60% at 00:00–03:00 and 16:00–19:00, respectively.

Studying the intervehicular distances is also important to identify the channel gain and the received power of the V2V-VLC link as indicated in (5), (10), and (11). The intervehicular

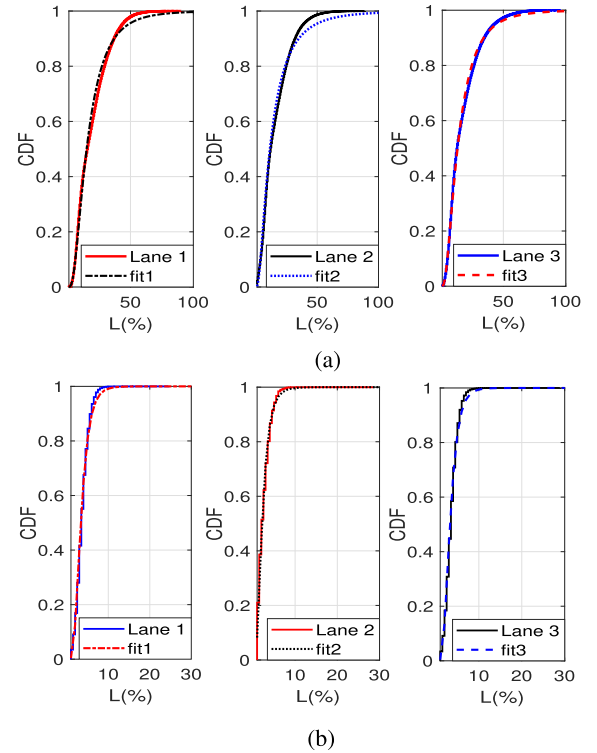


Fig. 5. CDFs of the coexistence of other vehicles in the adjacent lanes at (a) 00:00–03:00 and (b) 16:00–19:00.

distances change continuously due to the dynamic nature of vehicular traffic density during different periods of the day as well as with the lane. Similar to the coexistence of other vehicles cases, we performed a CDF curve fitting method with normal, log-normal, exponential, and Nakagami distributions to

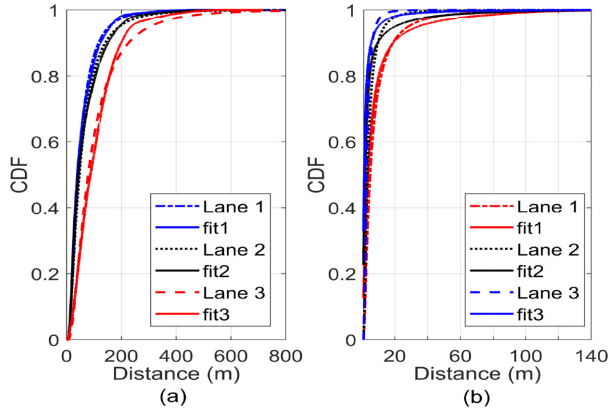


Fig. 6. CDFs of the intervehicular distances in the three lanes at (a) 00:00–03:00 and (b) 16:00–19:00.

establish the distribution that closely estimates intervehicle distance. Table I summarizes the estimation standard error values for these distributions for the three lanes during 00:00–03:00 and 16:00–19:00 hours. The table shows that the log-normal distribution has the least estimation error value. This is consistent with the literature, which reported that the log-normal distribution offers a close fit to the intervehicle distance [32]–[34]. Hence, the distribution of the intervehicular distances is given by

$$P_D(d) = \frac{1}{\delta_d \sqrt{2\pi}} \frac{1}{d} \exp\left(-\frac{(\ln(d) - \mu_d)^2}{2\delta_d^2}\right). \quad (17)$$

The distribution parameters  $\mu_d$  and  $\delta_d$  are given in Table I. The CDFs of the intervehicular distances and a log-normal distribution for the three lanes during 00:00–03:00 and 16:00–19:00 are depicted in Fig. 6.

### B. V2V-VLC Link Performance Results

The channel quality metrics SNR and the corresponding BER performance of the V2V-VLC link was simulated using the parameters summarized in Table II. The BER performance is evaluated with regard to the transmit SNR to examine the impact of channel path loss variation during different periods of the day. Evaluating system performance in terms of transmit SNR is a standard method in VLC, especially when the channel impulse response is varying [35]–[38]. Considering received power in (5) and the SNR at the receiver in (7), the transmit SNR is given by

$$\text{SNR}_T[\text{dB}] = 10 \log\left(\frac{\gamma^2 H(0)^2 P_T^2}{\sigma_T^2}\right) - 10 \log(H(0)^2). \quad (18)$$

Therefore, the SNR values (in dB) at the receiver are offset by the corresponding channel path loss values [35]. The simulation is carried out for a transmitter vehicle and a receiver vehicle separated by an intervehicular distance  $D$  with a mean value that changes according to transmitter–receiver vehicles' positions on different lanes and during different periods of the day (see Table I). The communication link is affected by

TABLE II  
SIMULATION PARAMETERS

Symbol	Parameter	Values
$P_T$	Transmitted power (normalized)	1 W
$\Phi_c$	Semi-angle	30° [23]
$\gamma$	PD responsivity	0.54 A/W [39]
$\Psi_c$	The receiver field of view	80° [3]
$A_r$	Receiver area	$1 \times 10^{-4} \text{ m}^2$ [3]
$C_{pd}$	Capacitance of PD per unit area	$1.12 \mu\text{Fm}^{-2}$ [18]
$I_2$ and $I_3$	Noise bandwidth factors	0.562 and 0.0868 [11]
$B_w$	Noise bandwidth	100 MHz [11]
$G_\nu$	Open-loop voltage gain	10 [18]
$\Gamma$	FET channel noise factor	1.5 [18]
$g_m$	FET transconductance	30 mS [18]
$I_{bg}$	Background current at $\lambda = 850 \text{ nm}$	55.4 $\mu\text{A}$ [11]
$\rho$	Reflection coefficient	0.8 [3]

the existence of three (i.e.,  $j = 1, 2,$  and  $3$ ) potential reflectors/interferers vehicles on the adjacent lanes located at  $(x_j, y_j)$  of  $(1, D/3) \text{ m}$ ,  $(0.5, D/2) \text{ m}$ , and  $(2, 2D/3) \text{ m}$  as illustrated in Fig. 1(b). However, demand from different lane can be considered by varying the angles  $\phi, \theta, \phi_s,$  and  $\theta_R$  in (10) and (12) to study other scenarios, as shown in Fig. 3.

BER performance of the V2V-VLC link in each of the three lanes between 00:00 and 03:00 is shown in Fig. 7(a) and (b), where Fig. 7(a) represents the asymmetrical radiation pattern of the low-beam and Fig. 7(b) represents the symmetrical radiation pattern of the high-beam headlights. The BER performance is estimated using a pseudorandom sequence of  $10^7$  bits length and a transmission rate of 50 Mbps assuming OOK modulation. The figures illustrate the BER performance of LOS components and NLOS components (i.e., excluding the LOS signal), which are reflected from the vehicles in the adjacent lanes. The figures show a large variation of the BER performance over different lanes. This is expected as the transmission distance in different lanes has different lane-dependent mean values as summarized in Table I. During the off-peak hours 00:00–03:00, the left-hand lane (Lane 1) has the shortest transmission distance with a mean value of 57.2 m compared to the mean values of the intervehicular distances of 67.1 m and 109.8 m for the middle lane (Lane 2) and the right-hand lane (Lane 3), respectively. Hence, the left-hand lane (Lane 1) has the least path loss and the highest SNR. Therefore, the BER values on this lane are lower than the middle and right-hand lanes (Lane 2 and 3). For example, at SNR = 130 dB, the BER values of the LOS link are 0.452, 0.101, and 0.003 for right-hand lanes (Lane 3), middle lane (Lane 2), and the left-hand lane (Lane 1), respectively. Furthermore, the BER values of the NLOS component for left-hand lane (Lane 1) is lower than the middle and right-hand lanes (Lane 2 and 3), e.g. at SNR = 205 dB, the BER values of the NLOS links are 0.49, 0.38, and 0.07 for right-hand lanes (Lane 3), middle lane (Lane 2), and the left-hand lane (Lane 1),

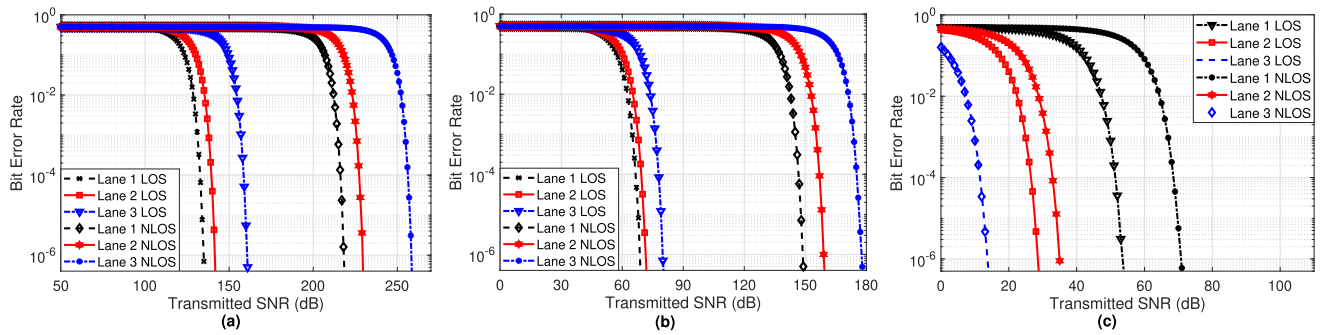


Fig. 7. BER performance of the V2V-VLC link in three lanes during (a) 00:00–03:00 when low-beam and (b) 00:00–03:00 when high-beam and (c) 16:00–19:00 when low-beam radiation pattern are considered.

respectively. Fig. 7(b) shows that at SNR = 60 dB, the BER values of the LOS links are 0.31, 0.10, and 0.04 for the right-hand lane (Lane 3), middle lane (Lane 2), and left-hand lanes (Lane 1), respectively. Hence, the V2V-VLC system is practically feasible when the high-beam is used. The figures show a large difference between the BER performance of the LOS component and the NLOS component as it is expected in Table I because the mean value of the probability of the coexistence of other vehicles in the adjacent lanes does not exceed 3.74%, i.e., the probability of reflection occurrence is very low.

BER performance of the V2V-VLC link in the three lanes at rush hours (16:00–19:00) is shown in Fig. 7(c). The figure shows that the BER performance of right-hand lane (Lane 3) is better than the middle and left-hand lanes (Lane 2 and 1). For example, at SNR = 10 dB, the BER values are 0.489, 0.290, and 0.001 for left-hand lanes (Lane 1), middle lane (Lane 2), and the right-hand lane (Lane 3), respectively. This is expected as the right-hand lane (Lane 3) has the shortest intervehicular distance with a mean value of 2.48 m during rush hours compared to the mean values of 3.93 m, and 7.79 m for middle lane (Lane 2), and the left-hand lane (Lane 1), respectively (see Table I). The BER values of the LOS and NLOS links are close for the right-hand lane (Lane 3). The difference in the BER performance of the NLOS and the LOS links increases in the middle lane (Lane 2) and the left-hand lane (Lane 1). The adequate performance of NLOS component is also expected from Section V-A due to the high probability of the co-existence of other vehicles in the adjacent lanes which can reach 90%, i.e., the probability of reflection occurrence is high.

Fig. 7 also shows that the required SNR ranges vary widely from hundreds of decibels during the off-peak hours to tens of decibels during the rush hours to achieve comparable BER values. This indicates the variation and dependency of channel capacity on the traffic conditions during different periods of the day. In addition, the figures examined the BER performance of the V2V-VLC system for a range of the transmitted SNR between 0 and 260 dB, similar to [35]–[38] where the transmitted SNR values ranged from 80 to 240 dB for an indoor environment when the transmission distance does not exceed 5 m. The transmitted SNR depends on the illumination level requirements. The actual SNR depends on a number of factors such as transmitter and receiver technology, data rate, optical gain, and optical filters. However, to fulfil illumination constraints,

TABLE III  
SUMMARY OF THE REQUIRED SNR VALUES TO ACHIEVE BER=10<sup>-6</sup> FOR DIFFERENT LAMPS, LANES, AND PROPAGATION PATH

Time		00:00-03:00				16:00-19:00	
		high-beam		low-beam		low-beam	
Path		LOS	NLOS	LOS	NLOS	LOS	NLOS
SNR (dB)	left (1)	68.6	148.7	134.8	218.2	53.6	70.8
	middle (2)	71.5	159.0	141.5	229.3	28.6	35.0
	right (1)	79.9	177.7	160.7	258.3	13.7	13.5

the transmitted optical power is a constant i.e., the transmitter SNR is fixed for a given system. Consequently, depending upon the transmitter SNR, the BER values change. This is a common challenge in mobile communication links. To ensure a minimum of communication requirements, various techniques such as automatic gain control, adaptive data rate, and rate-adaptive modulation are used [40], [41].

Table III provides a summary of the required SNR (at the transmitter) values to achieve a BER of 10<sup>-6</sup> for different lamps, lanes, and propagation paths. The table shows that higher SNR values are required to achieve acceptable BER performance at off-peak hours regardless of the propagation path (i.e., LOS or NLOS) compared to the rush hours. This is because the average inter-vehicular distance is lower during the rush hours compared to the late hours. The table also shows that communication using the NLOS path is feasible during rush hour. This is an important observation as the blocking probability of the LOS is significantly higher during the rush hours. However, the V2V-VLC is still feasible with only NLOS. In late hours, the blocking probability is less and LOS is available. This indicates that V2V-VLC is available for both rush and off-peak hours. Furthermore, for the same channel condition, the SNR requirements for the high-beam radiation are lower than the low-beam. This is due to the directional radiation pattern of high-beam, which reduces the path loss.

## VI. CONCLUSION

This article presented the impact of dynamic traffic on the performance of V2V-VLC for different lanes on two U.K. motorways at different times of the day. Using traffic measurements, the average intervehicular distances were estimated and the BER performance was evaluated. The intervehicular distance depends

on the traffic conditions as well as on the lane. Therefore, the BER performance at different lanes was evaluated for different traffic conditions and lanes. During off-peak hours, the BER at the left-hand lane is the lowest compared to the middle and right-hand lanes. This is because the mean intervehicular distance in the left-hand lane is 57.2 m which is lower than 67.1 and 109.8 m for the middle and right-hand lanes, respectively. During the rush hours, the right-hand lane has lower BER values than those of the middle and the left-hand lanes because the inter-vehicular distance in this lane has a lower mean value of 2.48 m compared to 3.93 and 7.79 m for the middle and left-hand lanes, respectively. Considering a large variation of inter-vehicular distances between rush and off-peak hours, lower values of SNR are required during rush hours to achieve comparable BER performance e.g., at a BER of  $10^{-6}$  the SNR required at right-hand lane for LOS links are 13.7 and 160.7 dB at the rush and off-peak hours, respectively.

In addition, the study adopted a statistical modeling approach to model the probability of coexistence of other vehicles in adjacent lanes and the impact of reflection from these vehicles. The results revealed that the probability of coexistence of other vehicles in the adjacent lanes during the rush hours is as high as 90%, while it decays to less than 10% during off-peak traffic hours. Hence, the probability of reflection from the adjacent vehicles is high during rush hours. Therefore, the performance of NLOS components due to reflection is significant and comparable to the LOS component, i.e., SNR values of less than 70 dB are required to achieve a BER value of  $10^{-6}$ . However, the performance of NLOS components is insignificant during off-peak hours as the required SNR values to achieve  $BER = 10^{-6}$  are larger than 100 dB.

#### ACKNOWLEDGMENT

The authors would like to thank Highways England and Mott MacDonald for providing us with traffic data that were also used in the InnovateUK funded project UKCITE, grant 102581. This work was carried out as a self-funded PhD programme at Coventry University, UK. O Haas was funded by Assured CAV Parking, innovate-UK grant 105095, Cheng-Xiang Wang was funded by the National Natural Science Foundation of China (NSFC) under Grant 61960206006 and the EU H2020 RISE TESTBED2 project under Grant 872172.

#### REFERENCES

- [1] World Health Organization, "Global Status Report on Road safety 2018," no. 9789241565684, 2018. [Online]. Available: <https://www.who.int/publications/i/item/9789241565684>
- [2] S. Rehman, S. Ullah, P. Chong, S. Yongchareon, and D. Komosny, "Visible light communication: A system perspective-overview and challenges," *Sensors*, vol. 19, no. 5, Mar. 2019, Art. no. 1153.
- [3] A. Al-Kinani, J. Sun, C. Wang, W. Zhang, X. Ge, and H. Haas, "A 2-D non-stationary GBMSM for vehicular visible light communication channels," *IEEE Trans. Wireless Commun.*, vol. 17, no. 12, pp. 7981–7992, Dec. 2018.
- [4] C. X. Wang, J. Huang, H. Wang, X. Gao, X. You, and Y. Hao, "6G wireless channel measurements and models: Trends and challenges," *IEEE Veh. Technol. Mag.*, vol. 15, no. 4, pp. 22–32, Dec. 2020.
- [5] Q. Chen, C. X. Wang, J. Sun, W. Zhang, and Q. Zhu, "A non-stationary VVLC MIMO channel model for street corner scenarios," in *Proc. Int. Wireless Commun. Mobile Comput.*, Limassol, Cyprus, 2020, pp. 365–370.
- [6] X. You *et al.*, "Towards 6G wireless communication networks: Vision, enabling technologies, and new paradigm shifts," *Sci. China Inf. Sci.*, vol. 64, no. 1, pp. 1–74, Jan. 2021.
- [7] M. Uysal, Z. Ghassemlooy, A. Bekkali, A. Kadri, and H. Menouar, "Visible light communication for vehicular networking: Performance study of a V2V system using a measured headlamp beam pattern model," *IEEE Veh. Technol. Mag.*, vol. 10, no. 4, pp. 45–53, Dec. 2015.
- [8] B. Béchadergue, L. Chassagne, and H. Guan, "Simultaneous visible light communication and distance measurement based on the automotive lighting," *IEEE Trans. Intell. Veh.*, vol. 4, no. 4, pp. 532–547, Aug. 2019.
- [9] J. Chen and Z. Wang, "Topology control in hybrid VLC/RF vehicular ad-hoc network," *IEEE Trans. Wireless Commun.*, vol. 19, no. 3, pp. 1965–1976, Mar. 2020.
- [10] L. U. Khan, "Visible light communication: Applications, architecture, standardization and research challenges," *Digit. Commun. Netw.*, vol. 3, no. 2, pp. 78–88, May. 2017.
- [11] Z. Ghassemlooy, W. Popoola, and S. Rajbhandari, *Optical Wireless Communications: System and Channel Modelling With Matlab*. Boca Raton, FL, USA: CRC Press, 2019.
- [12] G. Singh, A. Srivastava, and V. A. Bohara, "Impact of weather conditions and interference on the performance of VLC based V2V communication," in *Proc. Int. Conf. Transparent Opt. Netw.*, Angers, France, 2019, pp. 1–4.
- [13] I. E. Lee, M. L. Sim, and F. W. L. Kung, "Performance enhancement of outdoor visible-light communication system using selective combining receiver," *IET Optoelectron.*, vol. 3, no. 1, pp. 30–39, Feb. 2009.
- [14] M. S. Islam *et al.*, "The impact of solar irradiance on visible light communications," *J. Lightw. Technol.*, vol. 36, no. 12, pp. 2376–2386, Mar. 2018.
- [15] Y. H. Chung and S. Oh, "Efficient optical filtering for outdoor visible light communications in the presence of sunlight or artificial light," in *Proc. Int. Symp. Intell. Signal Process. Commun. Syst.*, Naha, Japan, 2013, pp. 749–752.
- [16] D. Cervinka, Z. Ahmad, O. Salih, and S. Rajbhandari, "A study of yearly sunlight variance effect on vehicular visible light communication for emergency service vehicles," in *Proc. 12th IEEE/IET Int. Symp. Commun. Syst. Netw. Digit. Signal Process.*, Porto, Portugal, 2020, pp. 1–6.
- [17] R. Khoder, R. Naja, and S. Tohme, "Impact of interference on visible light communication performance in a vehicular platoon," in *Proc. Int. Wireless Commun. Mobile Comput.*, Limassol, Cyprus, Jul. 2020, pp. 1935–1939.
- [18] P. Luo, Z. Ghassemlooy, H. L. Minh, E. Bentley, A. Burton, and X. Tang, "Performance analysis of a car-to-car visible light communication system," *Appl. Opt.*, vol. 54, no. 7, pp. 1696–1706, Mar. 2015.
- [19] P. Luo, Z. Ghassemlooy, E. Bentley, A. Burton, and X. Tang, "Bit-error-rate performance of a car-to-car VLC system using 2 MIMO," *Mediterranean J. Comput. Netw.*, vol. 11, pp. 400–407, Jan. 2015.
- [20] A. Al-Kinani *et al.*, "A 3D non-stationary GBMSM for vehicular visible light communication MISO channels," *IEEE Access*, vol. 8, pp. 140 333–140 347, 2020.
- [21] F. M. Alsalamy, Z. Ahmad, O. Haas, and S. Rajbhandari, "Regular-shaped geometry-based stochastic model for vehicle-to-vehicle visible light communication channel," in *Proc. IEEE Jordan Int. Joint Conf. Elect. Eng. Inf. Technol.*, Amman, Jordan, 2019, pp. 297–301.
- [22] F. M. Alsalamy *et al.*, "Impact of vehicle headlights radiation pattern on dynamic vehicular visible light communication system channel," *J. Lightw. Technol.*, vol. 39, no. 10, pp. 3162–3168, May 15, 2021.
- [23] F. M. Alsalamy, Z. Ahmad, S. Zvanovec, P. A. Haigh, O. C. Haas, and S. Rajbhandari, "Statistical channel modelling of dynamic vehicular visible light communication system," *Veh. Commun.*, vol. 29, Jun. 2021, Art. no. 100339. [Online]. Available: <https://www.sciencedirect.com/science/article/pii/S2214209621000085>
- [24] M. Rahaim and T. D. C. Little, "Interference in IM/DD optical wireless communication networks," *IEEE/OSA J. Opt. Commun. Netw.*, vol. 9, no. 9, pp. D 51–D63, Sep. 2017.
- [25] M. A. Esmail, H. Fathallah, and M. Alouini, "Outage probability analysis of FSO links over foggy channel," *IEEE Photon. J.*, vol. 9, no. 2, pp. 1–12, Apr. 2017.
- [26] F. Chen, K. Wang, Z. Qin, D. Wu, X. Luo, and S. Liu, "Design method of high-efficient LED headlamp lens," *Opt. Exp.*, vol. 18, no. 20, pp. 20 926–38, Sep. 2010.

- [27] *United Nations*, “United Nations Economic Commission for Europe Vehicle Regulations, Reg. 112-Rev.3,” UN, no. 9789241565684, Jan. 2013. [Online]. Available: <https://www.unece.org/fileadmin/DAM/trans/main/wp29/wp29regs/2013/R112r3e.pdf>
- [28] L. Cheng, W. Viriyasitavat, M. Boban, and H. Tsai, “Comparison of radio frequency and visible light propagation channels for vehicular communications,” *IEEE Access*, vol. 6, pp. 2634–2644, 2018.
- [29] A. Memedi, H. Tsai, and F. Dressler, “Impact of realistic light radiation pattern on vehicular visible light communication,” in *Proc. IEEE Global Commun. Conf.*, Singapore, 2017, pp. 1–6.
- [30] N. K. Akafuah, S. Poozesh, A. Salaimah, G. Patrick, K. Lawler, and K. Saito, “Evolution of the automotive body coating process—a review,” *Coatings*, vol. 6, no. 2, pp. 1–24, Jun. 2016.
- [31] R. Đuriković and T. Ágošton, “Prediction of optical properties of paints,” *Central Eur. J. Phys.*, vol. 5, no. 3, pp. 416–427, Sep. 2007.
- [32] I. Greenberg, “The log-normal distribution of headways,” *Australian Road Res.*, vol. 2, no. 7, pp. 14–18, Mar. 1966.
- [33] G. Yan and S. Olariu, “A probabilistic analysis of link duration in vehicular ad hoc networks,” *IEEE Trans. Intell. Transp. Syst.*, vol. 12, no. 4, pp. 1227–1236, Dec. 2011.
- [34] R. Roy and P. Saha, “Headway distribution models of two-lane roads under mixed traffic conditions: A case study from india,” *Eur. Transp. Res. Rev.*, vol. 10, no. 1, pp. 1–12, Mar. 2018.
- [35] H. Marshoud, P. C. Sofotasios, S. Muhaidat, G. K. Karagiannidis, and B. S. Sharif, “On the performance of visible light communication systems with non-orthogonal multiple access,” *IEEE Trans. Wireless Commun.*, vol. 16, no. 10, pp. 6350–6364, Oct. 2017.
- [36] P. M. Butala, H. Elgala, and T. D. C. Little, “Performance of optical spatial modulation and spatial multiplexing with imaging receiver,” in *Proc. Wireless Commun. Netw. Conf.*, Istanbul, Turkey, 2014, pp. 394–399.
- [37] C. Chen *et al.*, “User-centric MIMO techniques for indoor visible light communication systems,” *IEEE Syst. J.*, vol. 14, no. 3, pp. 3202–3213, Sep. 2020.
- [38] C. He, T. Q. Wang, and J. Armstrong, “Performance comparison between spatial multiplexing and spatial modulation in indoor MIMO visible light communication systems,” in *Proc. IEEE Int. Conf. Commun.*, 2016, pp. 1–6.
- [39] Y. H. Kim, W. A. Cahyadi, and Y. H. Chung, “Experimental demonstration of VLC-based vehicle-to-vehicle communications under fog conditions,” *IEEE Photon. J.*, vol. 7, no. 6, pp. 1–9, Dec. 2015.
- [40] A.-M. Căilean, M. Dimian, and V. Popa, “Noise-adaptive visible light communications receiver for automotive applications: A step toward self-awareness,” *Sensors*, vol. 20, no. 13, 2020, Art. no. 3764.
- [41] A. Căilean, M. Dimian, V. Popa, L. Chassagne, and B. Cagneau, “Novel DSP receiver architecture for multi-channel visible light communications in automotive applications,” *IEEE Sensors J.*, vol. 16, no. 10, pp. 3597–3602, May 2016.